Mineral Mapping with AVIRIS and EO-1 Hyperion

Fred A. Kruse[1]

1.0 Introduction

Imaging Spectrometry data or Hyperspectral Imagery (HSI) acquired using airborne systems have been used in the geologic community since the early 1980's and represent a mature technology (Goetz et al., 1985; Kruse et al., 1999). The solar spectral range, 0.4 to 2.5 µm, provides abundant information about many important Earth-surface minerals (Clark et al., 1990). In particular, the 2.0 to 2.5 µm (SWIR) spectral range covers spectral features of hydroxyl-bearing minerals, sulfates, and carbonates common to many geologic units and hydrothermal alteration assemblages. Previous research has proven the ability of airborne and spaceborne hyperspectral systems to uniquely identify and map these and other minerals, even in sub-pixel abundances (Kruse and Lefkoff, 1993; Boardman and Kruse, 1994; Boardman et al., 1995; Kruse, et al., 1999). This paper describes a case history for a site in northern Death Valley, California and Nevada along with selected SNR calculations/results for other sites around the world. Various hyperspectral mineral mapping results for this site have previously been presented and published (Kruse, 1988; Kruse et al., 1993, 1999, 2001, 2002, 2003), however, this paper presents a condensed summary of key details for hyperspectral data from 2000 and 2001 and the results of accuracy assessment for satellite hyperspectral data compared to airborne hyperspectral data used as ground truth.

2.0 Comparison of Hyperion and AVIRIS Specifications

The launch of NASA's EO-1 Hyperion sensor in November 2000 marked the establishment of spaceborne hyperspectral mineral mapping capabilities. Hyperion is a satellite hyperspectral sensor covering the 0.4 to 2.5 µm spectral range with 242 spectral bands at approximately 10nm spectral resolution and 30m spatial resolution from a 705km orbit (Pearlman et al., 1999). Hyperion is a pushbroom instrument, capturing 256 spectra each with 242 spectral bands over a 7.5Km-wide swath perpendicular to the satellite motion. The system has two grating spectrometers; one visible/near infrared (VNIR) spectrometer (approximately 0.4 – 1.0 µm) and one short-wave infrared (SWIR)) spectrometer (approximately 0.9 – 2.5 µm). Data are calibrated to radiance using both pre-mission and on-orbit measurements. Key AVIRIS and Hyperion characteristics are compared in Table 1 and discussed further in Green et al., 2003.

The Airborne Visible/Infrared Imaging Spectrometer (AVIRIS) represents the current state of the art airborne hyperspectal system. AVIRIS, flown by NASA/Jet Propulsion Laboratory (JPL) is a 224-channel imaging spectrometer with approximately 10 nm spectral resolution covering the 0.4 – 2.5 µm spectral range (Green et al., 1999). The sensor is a whiskbroom system utilizing scanning foreoptics to acquire cross-track data. The IFOV is 1 milliradian. Four off-axis double-pass Schmidt spectrometers receive incoming illumination from the foreoptics using optical fibers. Four linear arrays, one for each spectrometer, provide high sensitivity in the 0.4 to 0.7 µm, 0.7 to 1.2 µm, 1.2 to 1.8 µm, and 1.8 to 2.5 µm regions respectively. AVIRIS is flown as a research instrument on the NASA ER-2 aircraft at an altitude of approximately 20 km, resulting in approximately 20-m pixels and a 10.5-km swath width. Since 1998, it has also been flown on a Twin Otter aircraft at low altitude, yielding 2 – 4m spatial resolution.

Table 1: AVIRIS/Hyperion Sensor Characteristics Comparison

HSI Sensor	Spectral Resolution	Spatial Resolution	Swath Width	SWIR SNR
AVIRIS-High Altitude	10 nm	20 m	12 km	~500:1
Hyperion	10 nm	30 m	7.5 km	~50:1

[1] Analytical Imaging and Geophysics LLC (AIG), Boulder, Colorado, USA, E-mail: kruse@aigllc.com

3.0 Methods

Analytical Imaging and Geophysics LLC (AIG) has developed methods for analysis of hyperspectral data that allow reproducible results with minimal subjective analysis (Kruse et al., 1996, 2001). These approaches are implemented and documented within the "Environment for Visualizing Images" (ENVI) software system originally developed by AIG scientists (now an Eastman Kodak/Research Systems Inc [RSI] commercial-off-the-shelf [COTS] product) (Research Systems Inc, 2001). They are also described in additional detail in Kruse et al. (2002, 2003). The hyperspectral analysis methodology includes 1) data pre-processing (area-array destriping as required), 2) correction of data to apparent reflectance using the atmospheric correction software ACORN (AIG, 2001), 3) linear transformation of the reflectance data using a Minimum Noise Fraction (MNF) transform to minimize noise and determine data dimensionality (Green et al., 1988; Boardman 1993), 4) location of the most spectrally pure pixels using the Pixel Purity Index (PPI) approach (Boardman et al. 1994, 1995), 5) extraction of endmemember spectra using n-dimensional scatter plotting (Boardman et al., 1995), 6) identification of endmember spectra using visual inspection, automated identification, and spectral library comparisons (Kruse and Lefkoff, 1993; Kruse et al., 1993) and 7) spatial mapping and abundance estimates for specific image endmembers using the Mixture-Tuned Matched Filtering (MTMF) method (Boardman, 1998). A key point of this methodology is the reduction of data in both the spectral and spatial dimensions to locate, characterize, and identify a few key spectra (endmembers) that can be used to explain the rest of the hyperspectral dataset. Once these endmembers are selected, then their location and abundances can be mapped from the linearly-transformed or original data. These methods derive the maximum information from the hyperspectral data themselves, minimizing the reliance on *a priori* or outside information.

4.0 Results – Northern Death Valley Site

The study area described here is located in northern Death Valley, at the extreme northern end of Death Valley National Park (Figure 1). The geology consists principally of a Jurassic-age intrusion exhibiting quart-sericite-pyrite hydrothermal alteration (Wrucke et al., 1984; Kruse, 1988). This site has been used as a test area for imaging spectrometers since 1983 (Kruse, 1988; Kruse et al., 1993, 1999). For the purposes of this study, AVIRIS data collected 9 June 2000 (f000609t01p03_r04) were compared to Hyperion data collected July 23 2001 (EO12001204_20AD20AC_r1_PF1_01.L1_A).

Figure 1: Location of the Northern Death Valley Site

A spectral subset of bands covering the short wave infrared (SWIR) spectral range (2.0 – 2.5 μm for AVIRIS and 2.0 – 2.4 μm for Hyperion) was selected and these bands were linearly transformed using the MNF transformation. A plot of eigenvalues versus MNF band number (not shown) shows a sharp falloff in eigenvalue magnitude between 1 and 20 for AVIRIS and between 1 and 10 for Hyperion. Because higher eigenvalues generally indicate higher information content, this indicates that the AVIRIS data contain significantly more information. The actual data dimensionality is usually determined by comparing both the eigenvalue plots and the MNF images for each dataset (Figures 2 and 3). In the case of AVIRIS, the MNF analysis indicates a dimensionality of approximately 20. The Hyperion data exhibits dimensionality of approximately 8.

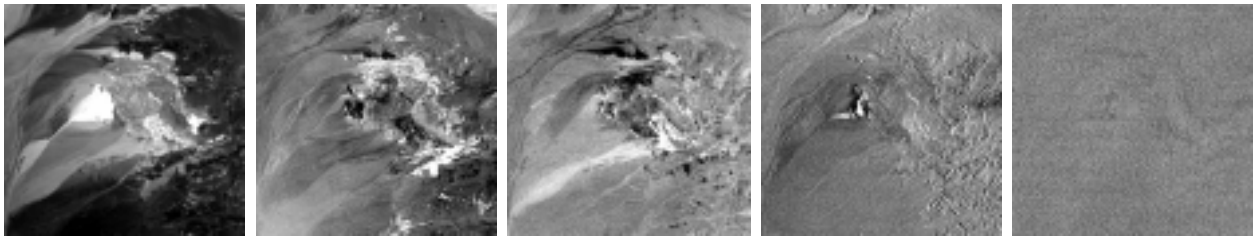

Figure 2. MNF images for the northern Death Valley AVIRIS SWIR data. Images from left to right, MNF band 1, MNF band 5, MNF band 8, MNF band 10, MNF band 20.

Figure 3. MNF images for the northern Death Valley Hyperion SWIR data. Images from left to right, MNF band 1, MNF band 5, MNF band 8, MNF band 10, MNF band 20.

The top MNF bands for each data set (20 for AVIRIS, 6 for Hyperion), which contain most of the spectral information (Green et al., 1988), were used to determine the most likely endmembers using the PPI procedure. These potential endmember spectra were loaded into an n-dimensional scatterplot and rotated in real time on the computer screen until "points" or extremities on the scatterplot were exposed (Boardman, 1993). These projections were "painted" using region-of-interest (ROI) definition procedures and then rotated again in 3 or more dimensions (3 or more MNF bands) to determine if their signatures were unique in the MNF data. Once a set of unique pixels were defined, then each separate projection on the scatterplot (corresponding to a pure endmember) was exported to a ROI in the image. Mean spectra were then extracted for each ROI from the apparent reflectance data to act as endmembers for spectral mapping (Figure 4). These endmembers were used for subsequent classification and other processing. Mixture-Tuned-Matched Filtering (MTMF), a spectral matching method (Boardman, 1998), was used to produce image-maps showing the distribution and abundance of selected minerals. (Note: MNF endmember spectra, not reflectance spectra are used in the MTMF). The results are generally presented as gray-scale images (not shown) with values from 0 to 1.0, which provide a means of estimating mineral abundance. Brighter pixels in the images represent higher mineral abundances. Results images for both AVIRIS and Hyperion were produced by correcting the Hyperion data to match the AVIRIS spatial scale and orientation as described above. Selected results were combined as color-coded images to show the distribution of the principal (spectrally predominant) minerals (Figures 5 and 6).

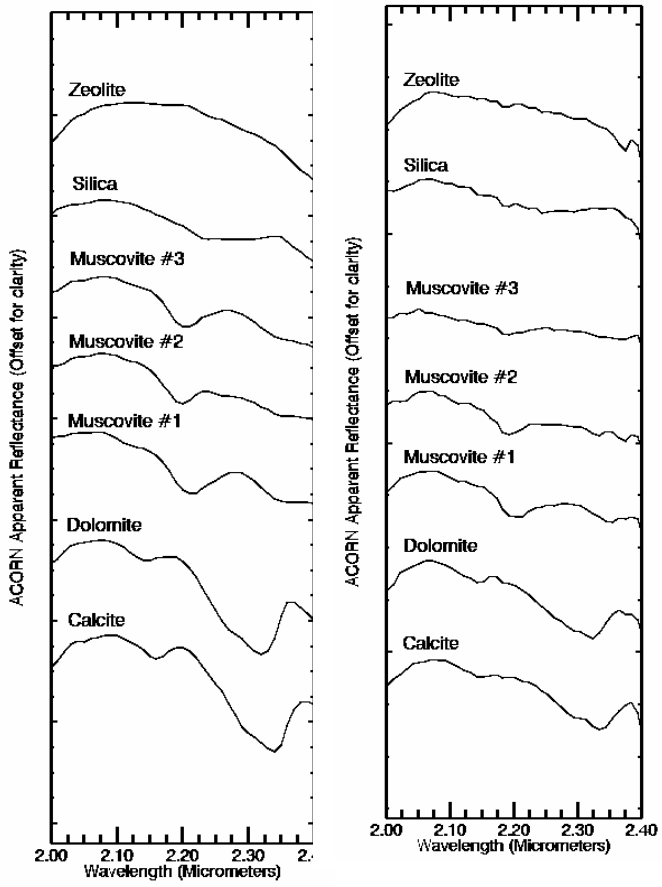

Figure 4: Comparison of selected AVIRIS endmember (mean) spectra (left) and Hyperion endmember (mean) spectra (right) for the northern Death Valley, California and Nevada site.

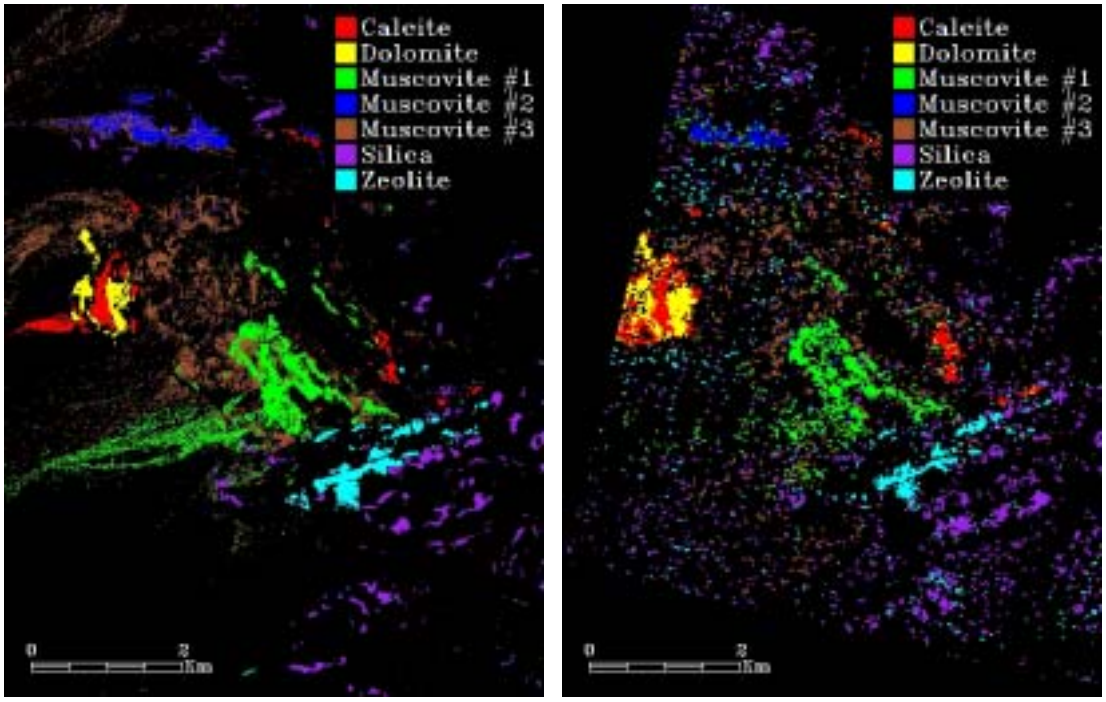

Figure 5: MTMF mineral maps for AVIRIS (left) and Hyperion (right) produced for the endmembers in Figure 4 for the northern Death Valley, California and Nevada site. Colored pixels show the spectrally predominant mineral at concentrations greater than 10%.

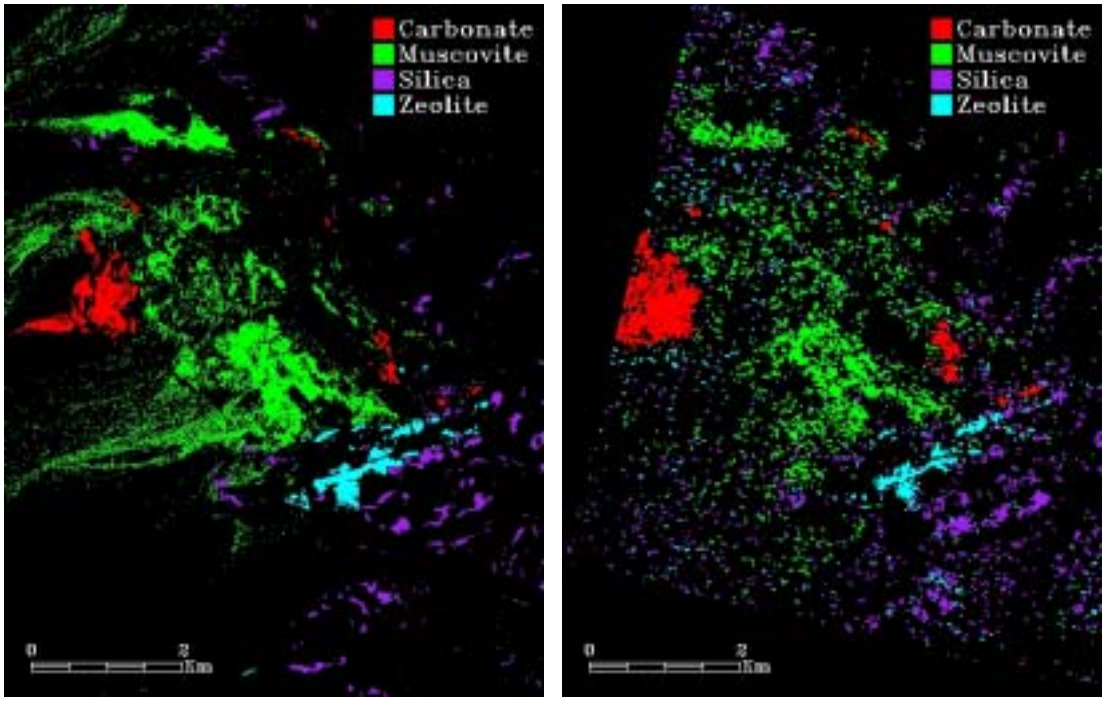

Figure 6: MTMF mineral maps for AVIRIS (left) and Hyperion (right) produced for a subset (combined) of the endmembers in Figure 4 for the northern Death Valley, California and Nevada site. Colored pixels show the spectrally predominant mineral group at concentrations greater than 10%.

Visual comparison of the detailed mapping results for the northern Death Valley site shows that Hyperion identifies similar minerals to AVIRIS and that there is generally good correspondence between the AVIRIS and Hyperion mapping. It is also possible to extract abundance information from both the AVIRIS and Hyperion data (Boardman and Kruse, 1994; Boardman et al., 1995, Kruse et al, 1999), but this is not illustrated here. Confusion matrix results comparing the AVIRIS and Hyperion mapping results, excluding the unclassified pixels show overall accuracy of approximately 76% for the Hyperion mapping as compared to AVIRIS, with a Kappa Coefficient of 0.71. Table 2 indicates that there is, however, considerable difficulty separating similar mineralogy. In this case, detecting and mapping the three muscovite varieties appears to be near the detection limit at the calculated 60:1 SNR of the Hyperion data. Grouping similar minerals together (calcite with dolomite, and combining the three muscovites) results in dramatic identification and mapping improvements (Figure 6, Table 3).

Table 2: Confusion Matrix comparing Hyperion northern Death Valley MTMF mineral mapping results to AVIRIS "Ground Truth" MTMF detailed mineral mapping results. Excludes unclassified pixels. Overall Accuracy is 76%. Kappa coefficient is 0.71

	AVIRIS Ground Truth (Percent)							
Hyperion Class	Calcite	Dolomite	Muscovite #1	Muscovite #2	Muscovite #3	Silica	Zeolite	Total
Calcite	**82.66**	16.75	0.00	0.31	1.11	0.46	0.21	11.46
Dolomite	15.73	**83.01**	0.00	0.00	0.00	0.09	0.10	9.74
Muscovite	0.10	0.00	**85.62**	15.04	41.13	1.37	0.00	33.07
Muscovite	0.00	0.00	2.11	**76.43**	11.49	0.09	0.00	8.62
Muscovite	0.10	0.00	8.33	4.50	**35.65**	2.46	0.72	10.14
Silica	0.20	0.24	3.81	3.72	6.36	**89.70**	6.00	14.76
Zeolite	1.21	0.00	0.13	0.00	4.26	5.83	**92.96**	12.21
Total	100.00	100.00	100.00	100.00	100.00	100.00	100.00	100.00

Table 3: Confusion Matrix comparing Hyperion northern Death Valley MTMF mapping results to AVIRIS "Ground Truth" MTMF basic (Combined Minerals) mapping results. Excludes unclassified pixels. Overall Accuracy is 94%. Kappa coefficient is 0.91.

	AVIRIS Ground Truth (Percent)				
Hyperion Class	Carbonate	Muscovite	Silica	Zeolite	Total
Carbonate	**99.01**	0.44	0.55	0.31	21.19
Muscovite	0.11	**93.23**	3.92	0.72	51.83
Silica	0.22	4.72	**89.70**	6.00	14.76
Zeolite	0.66	1.61	5.83	**92.96**	12.21
Total	100.00	100.00	100.00	100.00	100.00

5.0 SNR Comparisons – Effect on Mineral Mapping

The quality of digital remote sensing data is directly related to the level of system noise relative to signal strength. This is usually expressed as Signal-to-Noise Ratio (SNR), a dimensionless number that describes overall system radiometric performance (Collwell, 1983). System noise is tied to sensor design and takes into account factors such as detector performance/sensitivity, spatial/spectral resolution, and noise characteristics of the system electronics. Though the noise levels for a given sensor are generally fixed, for remote sensing data acquisition, the signal portion of the SNR is affected by other external factors such as solar zenith angle, atmospheric attenuation and scattering, and surface reflectance, which modify the signal available to the sensor (Collwell, 1983).

One common means for determining an approximate SNR for remote sensing data is to use a Mean/Standard Deviation method (Green et al., 1999, 2003). This approach requires definition of a spectrally homogeneous area, calculation of the average spectrum for that area, and determination of the spectrally distributed standard deviation for the average spectrum. SNR are normalized to 50% reflectance for comparison. SNR calculated using this method are representative of those that can be extracted directly from the data, however, SNR for bright targets may be underestimated because of homogeneity issues at higher SNR (increasing SNR may result in breakdown of apparently homogeneous areas into multiple materials and new homogeneous areas must be selected). Slightly higher SNR values could probably be obtained through direct analysis of the data dark current signal (Green et al., 1999), an "Instrument SNR", however, this isn't always possible. SNR calculated using the Mean/Standard Deviation method, an "Environmental SNR" are sensitive to acquisition conditions as mentioned above, and thus should be considered lower limits on performance.

Analysis of approximately 14 Hyperion scenes from around the world using the Mean/Standard Deviation SNR method shows that there is a strong relationship between the acquisition time of year (which controls the solar zenith angle) and the SNR of the Hyperion data (Kruse et al., 2001, 2003). Calculated SNR for Hyperion SWIR data are higher in the summer and lowest in the winter (Figure 7). This has a direct effect on spectral mineral mapping, with lower SWIR SNR resulting in extraction of less detail (Kruse et al., 2001, 2002, 2003). While Hyperion data with approximately 25:1 SNR allow basic mineral identification (no separation of within-species variability) more detail (additional endmembers) are detected and mapped using the higher SNR AVIRIS and Hyperion data (60:1 SNR) at the northern Death Valley site. This is also important for geologic/mineral mapping, because higher SNR allows separation of similar endmembers such as calcite from dolomite (Figure 4) and within-species variability such as kaolinite vs dickite (Figure 4). In the northern Death Valley case, the relatively high Hyperion SNR allows detection of 3 different mica endmembers with different aluminum substitution (Kruse et al., 1999). Previous investigations have indicated that SNR is critical for this determination (Kruse, 1988, Kruse et al., 2002).

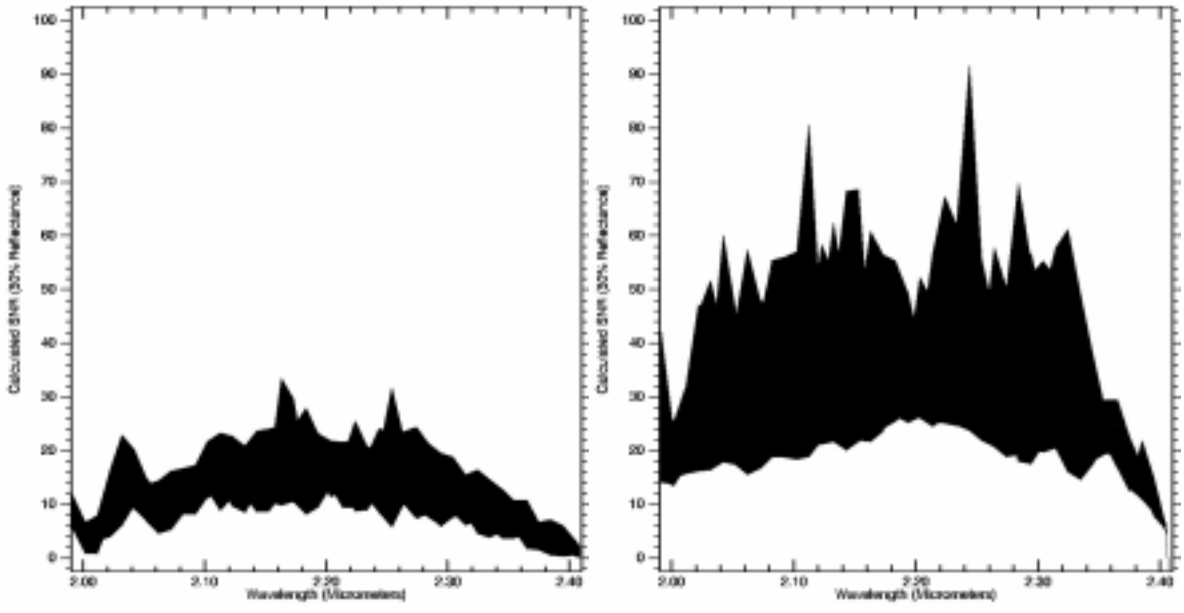

Figure 7: Comparison of Hyperion calculated SNR for "winter" data (left) and "summer" data (right). Filled areas indicate range of SNR for 14 Hyperion scenes.

6.0 Conclusions

Results at the northern Death Valley site establishes that data from the Hyperion SWIR spectrometer (2.0 – 2.4 μm) can be used to produce useful geologic (mineralogic) information. Comparison of Hyperion data to airborne hyperspectral data (AVIRIS) show that Hyperion provides the ability to remotely map basic surface mineralogy. Minerals mapped at this site include calcite, dolomite, muscovite (3 varieties), hydrothermal silica, and zeolites. These case histories demonstrate the analysis methodologies and level of information available from these Hyperion data. They also demonstrate the viability of Hyperion as a means of extending hyperspectral mineral mapping to areas not accessable to aircraft sensors.

AVIRIS data collected during July 2000 (northern Death Valley) served as the "ground truth" for this investigation. Comparison of Hyperion results for northern Death Valley (June 2001) to the known mineralogy derived from the AVIRIS data generally validate on-orbit mineral mapping and Hyperion performance. Standardized hyperspectral data processing methods applied to the Hyperion data lead to definition of specific key minerals, however, it is more difficult (than for AVIRIS) to extract the information because of the Hyperion data's lower SNR. The effect of this reduced response compared to AVIRIS is lower data dimensionality, thus fewer endmembers can be identified and mapped than with AVIRIS. Accuracy assessment and error analysis indicates that with Hyperion data that, in many cases, mineral identification is not possible where specific minerals are known to exist. In addition, Hyperion often confuses similar minerals that are separable using AVIRIS

The Hyperion data demonstrate the importance of high signal-to-noise performance for hyperspectral sensors. The northern Death Valley Hyperion scene was collected under optimum (summer – high solar zenith angle) conditions and exhibits SWIR SNR as high as approximately 60:1. These data allow detailed mineral mapping, including within-species variability, however, this capability is at the detection limit of current Hyperion SNR levels. Combining minerals to form a basic mineral map results in improved mapping with greater than 94% correspondence between AVIRIS and Hyperion at the northern Death Valley site. The level of mineralogic information available from the Hyperion data is directly tied to the SNR.

As a technology demonstration, Hyperion performs satisfactorily for mineral identification and mapping. Summer season Hyperion acquisitions with high SNR result in improved mapping capabilities. Improvements principally take the form of characterizing subtle distinctions such as determining the difference between calcite and dolomite and mapping within-species variability caused by molecular substitution (eg: aluminum substitution in micas). Unfortunately, Hyperion data collected under less than optimum conditions (winter season, dark targets) have marginal SWIR SNR and allow mapping of only the most basic mineral occurrences and mineral differences. This results in a recommendation that future HSI satellite sensors have significantly higher SNR performance specifications than Hyperion for the SWIR (at least 100:1 based on dark current measurements).

7.0 Acknowledgments

This research was partially funded by NASA under grant NCC5-495. Additional financial support was provided by Analytical Imaging and Geophysics LLC internal research and development funds. AVIRIS data were provided by JPL. ACORN is a trademark of ImSpec Associates, LLC. ENVI is a registered trademark of Research Systems Inc., Boulder, Colorado. Pixel Purity Index (PPI), n-Dimensional Visualizer, Spectral Analyst, and Mixture-Tuned Matched Filter (MTMF) are all trademarks of Research Systems Inc.

8.0 References

Analytical Imaging and Geophysics LLC (AIG), 2001, *ACORN User's Guide, Stand Alone Version: Analytical Imaging and Geophysics LLC*, 64 p.

Boardman, J. W., 1993, Automated spectral unmixing of AVIRIS data using convex geometry concepts: in *Summaries, Fourth JPL Airborne Geoscience Workshop*, *JPL Publication 93-26*, v. 1, p. 11-14.

Boardman J. W., and Kruse, F. A., 1994, Automated spectral analysis: A geologic example using AVIRIS data, north Grapevine Mountains, Nevada: in *Proceedings, Tenth Thematic Conference on Geologic Remote Sensing,* Environmental Research Institute of Michigan, Ann Arbor, MI, p. I-407 - I-418.

Boardman, J. W., Kruse, F. A., and Green, R. O., 1995, Mapping target signatures via partial unmixing of AVIRIS data: in *Summaries, Fifth JPL Airborne Earth Science Workshop, JPL Publication 95-1*, v. 1, p. 23-26.

Boardman, J. W., 1998, Leveraging the high dimensionality of AVIRIS data for improved sub-pixel target unmixing and rejection of false positives: mixture tuned matched filtering, in: *Summaries of the Seventh Annual JPL Airborne Geoscience Workshop*, Pasadena, CA, p. 55.

Clark, R. N., King, T. V. V., Klejwa, M., and Swayze, G. A., 1990, High spectral resolution spectroscopy of minerals: *Journal of Geophysical Research*, v. 95, no. B8, p. 12653-12680.

Collwell, R. N. (ed.), 1983, Manual of Remote Sensing, 2nd Edition, American Society of Photogrammetry and Remote Sensing (ASPRS), pp. 344-363, and pp. 1196.

Goetz, A. F. H., G. Vane, J. E. Solomon, and B. N. Rock, 1985. Imaging spectrometry for earth remote sensing, *Science*, v. 228, p. 1147 - 1153.

Green, A. A., Berman, M., Switzer, B., and Craig, M. D., 1988, A transformation for ordering multispectral data in terms of image quality with implications for noise removal: *IEEE Transactions on Geoscience and Remote Sensing*, v. 26, no. 1, p. 65 - 74.

Green, R. O., B. Pavri, J. Faust, and O. Williams, 1999, "AVIRIS radiometric laboratory calibration, inflight validation, and a focused sensitivity analysis in 1998," in *Proceedings of the 8th JPL Airborne Earth Science Workshop: Jet Propulsion Laboratory Publication 99-17*, p. 161 – 175.

Green, R. O., Chrien, T. G., and Pavri, B., 2003, "On-orbit Determination of the Radiometric and Spectral Calibration of Hyperion Using Ground, Atmospheric and AVIRIS Underflight Measurements," *TGARS Special Issue on EO-1* (in press).

Kruse, F. A., 1988, Use of Airborne Imaging Spectrometer data to map minerals associated with hydrothermally altered rocks in the northern Grapevine Mountains, Nevada and California: *Remote Sensing of Environment*, v. 24, no. 1, pp. 31-51.

Kruse, F. A., and Lefkoff, A. B., 1993, Knowledge-based geologic mapping with imaging spectrometers: *Remote Sensing Reviews*, Special Issue on NASA Innovative Research Program (IRP) results, v. 8, p. 3 - 28.

Kruse, F. A., Lefkoff, A. B., and Dietz, J. B., 1993, Expert System-Based Mineral Mapping in northern Death Valley, California/Nevada using the Airborne Visible/Infrared Imaging Spectrometer (AVIRIS): *Remote Sensing of Environment, Special issue on AVIRIS, May-June 1993*, v. 44, p. 309 - 336.

Kruse, F. A., Huntington, J. H., and Green, R. O, 1996, Results from the 1995 AVIRIS Geology Group Shoot: in *Proceedings, 2nd International Airborne Remote Sensing Conference and Exhibition*: Environmental Research Institute of Michigan (ERIM), Ann Arbor, v. I, p. I-211 - I-220.

Kruse, F. A., Boardman, J. W., and Huntington, J. F., 1999, Fifteen Years of Hyperspectral Data: northern Grapevine Mountains, Nevada: in Proceedings of the 8th JPL Airborne Earth Science Workshop: Jet Propulsion Laboratory Publication, *JPL Publication 99-17*, p. 247 - 258.

Kruse, F. A., Boardman, J. W., and Huntington, J. F., 2001, Progress Report: Geologic Validation of EO-1 Hyperion: in Proceedings of the 10th JPL Airborne Earth Science Workshop: Jet Propulsion Laboratory Publication 02-1, p. 253 – 265.

Kruse, F. A., Boardman, J. W., and Huntington, J. F., 2002, "Comparison of EO-1 Hyperion and Airborne Hyperspectral Remote Sensing Data for Geologic Applications," in *Proceedings, SPIE Aerospace Conference, 9-16 March 2002, Big Sky, Montana*, published on CD-ROM, IEEE Catalog Number 02TH8593C, Paper #6.0102, 12 p.

Kruse, F. A., Boardman, J. W., Huntington, J. F., Mason, P., and Quigley, M.A., 2003, Evaluation and Validation of EO-1 Hyperion for Geologic Mapping: in Special Issue, TGARSS, IEEE (in press)

Pearlman, J., Stephen Carman, Paul Lee, Lushalan Liao and Carol Segal, 1999, Hyperion Imaging Spectrometer on the New Millennium Program Earth Orbiter-1 System: In Proceedings, International Symposium on Spectral Sensing Research (ISSSR), Systems and Sensors for the New Millennium, published on CD-ROM, International Society for Photogrammetry and Remote Sensing (ISPRS).

Research Systems Inc (RSI), 2001, ENVI User's Guide, Research Systems Inc, 948 p.

Wrucke, C. T., Werschkey, R. S., Raines, G. L., Blakely, R. J., Hoover, D. B, and Miller, M. S., 1984, "Mineral resources and mineral resource potential of the Little Sand Spring Wilderness Study Area, Inyo County, California," U. S. Geological Survey Open File Report 84-557, 20 p.